INSTITUTE OF PHYSICS PUBLISHING PLASMA PHYSICS AND CONTROLLED FUSION

Plasma Phys. Control. Fusion **46** (2004) 669–679 PII: S0741-3335(04)71845-X

Turbulence and transport in the scrape-off layer TCABR tokamak

A A Ferreira[1], M V A P Heller[1], I L Caldas[1], E A Lerche[1], L F Ruchko[1] and L A Baccalá[2]

[1] Institute of Physics, University of São Paulo, C. P. 66318, 05315-970 São Paulo, SP, Brazil
[2] Escola Politécnica, University of São Paulo, 05508-900 São Paulo, SP, Brazil

Received 11 November 2003
Published 16 March 2004
Online at stacks.iop.org/PPCF/46/669 (DOI: 10.1088/0741-3335/46/4/007)

Abstract

We study the scrape-off layer turbulence and transport in Tokamak Chauffage Alfvén Brésilien (TCABR) before and during the launching of radio frequency excited waves that interact with the boundary plasma. We present the main characteristics of the background electrostatic fluctuations and the intermittent bursts. During the perturbation, the plasma turbulence intensity increases and the average phase velocity reverses its direction. The total turbulence driven transport and the transport radially convected by the intermittent fluctuation bursts also increase with the perturbation. The probability distributions of the bursts have long tails, resembling those typical of flight distributions with a decay parameter increasing with the wave excitation.

1. Introduction

The interest in plasma edge turbulence in tokamaks is based on the evidence that in many experiments plasma edge behaviour influences the plasma confinement [1, 2]. Experiments indicate that anomalous edge particle transport is caused by diffusion, induced by a background electrostatic turbulence [1–3], and convection, produced by intermittent bursts independent of the background and associated to electrostatic structures [4–10]. Since these processes are not yet well understood, it is still important to investigate them in a variety of plasma conditions [3, 11].

We analyse turbulence and transport properties before and during the launching of radio frequency (rf) excited waves that interact with the boundary in Tokamak Chauffage Alfvén Brésilien (TCABR). The plasma condition before perturbation is typical of that obtained for Ohmically heated tokamaks. Another condition is obtained by externally injecting Alfvén waves into the plasma using a rf antenna for plasma heating and non-inductive current drive [12, 13]. In our experiment, we use a particular arrangement of these facilities to investigate the scrape-off layer turbulence modifications introduced by the rf injection. In this regime the plasma scrape-off layer response is mainly due to interaction of the excited

waves with the boundary plasma. We study how the rf injection affects the total transport in the scrape-off layer and the part of this transport carried out by intermittent convection due to bursts propagating radially. As in other tokamaks [14], in TCABR Alfvén waves have been used to generate the non-inductive current drive [13].

Meanwhile, some plasma conditions have been proposed to control plasma edge turbulence and transport [3]. In the DITE tokamak [15], for example, experiments with electron cyclotron waves produce plasma core modifications that affect the plasma boundary, increasing edge fluctuations and transport. Active feedback was used to modify the edge fluctuation spectrum of TEXT [16]. The background turbulence was reduced or enhanced depending on the phase shift and gain of the feedback network. One possibility is to use rf waves in tokamaks to induce changes in plasma turbulence and create transport barriers where the total transport is depressed [3]. Evidence that a flow-shear-induced transport barrier can be produced in core plasma using injected rf waves was found in the Princeton Beta Experiment Modification (PBX-M) [17].

We use a system of probes that measures simultaneously the electrostatic fluctuations and some plasma mean parameters (density, electron temperature and plasma potential) [18]. The study of turbulence is based on digital correlation techniques applied to the fluctuating potential and the ion saturation current [19].

Furthermore, to detect evidence of phase coupling between wavelet components of different scale lengths, possibly present in turbulence [20–22], we calculate wavelet bispectra of two frequencies and their sum or difference frequencies [18, 20–23]. The integrated bicoherences show episodes of significant non-linear interaction among broadband components of the wave number or frequency spectra.

The launching of Alfvén waves modifies not only the power spectra but also shows a substantial influence on the large fluctuation amplitude events and on the convection transport they produce.

This paper is organized as follows: the experiment is briefly described in section 2, power spectra and transport alterations are described and discussed in sections 3 and 4. The bursts, their amplitude, velocity and transport distributions are presented in section 5. The conclusion is given in section 6.

2. Experiment

The experiment is performed in a hydrogen circular plasma in TCABR [24] (major radius $R = 0.61$ m and minor radius $a = 0.18$ m). The plasma current is 100 kA, the current duration 100 ms, the hydrogen filling pressure 3×10^{-4} Pa, and toroidal magnetic field $B_t = 1.1$ T. The probe system is installed in the equatorial region of the tokamak, 90° from the limiter in the toroidal direction. The multipin Langmuir probe is composed of a triple probe that measures the mean density, plasma potential, and electron temperature; two pins measure the fluctuations of the floating potential and a third one measures ion saturation current fluctuations. The probes mounted on a movable shaft can be moved radially from $r = 15 \times 10^{-2}$ to 23×10^{-2} m (distance referred to the centre of the plasma column) in separate discharges [18]. The time series measurements are recorded using ADC in a VME board with 12-bit digitizers, at a sampling rate of 1 MHz. The bandwidth of the measuring circuit is approximately 300 kHz to avoid alaising. Thus, we typically analyse 50 000 points in every discharge. Although the noise on probe data increases with rf waves, it is at least an order of magnitude lower than that of the plasma fluctuation level.

We investigate the scrape-off layer turbulence and transport changes introduced by the rf power coupled to the plasma during the Alfvén wave excitation pulse. The complete description

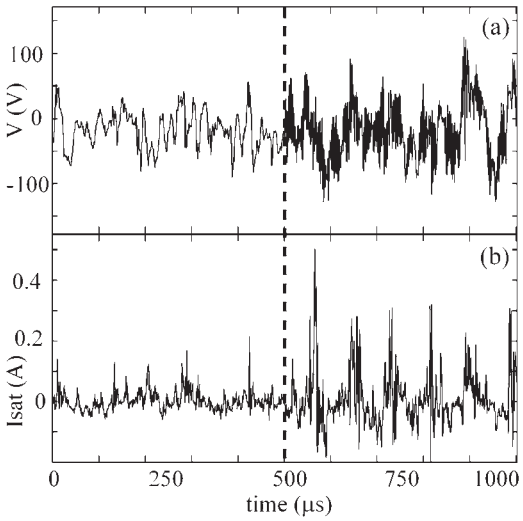

Figure 1. A chosen region of the floating potential (*a*) and ion saturation current fluctuations (*b*) without and with (after dashed line) rf injection.

of the rf system is given in [12] and the results obtained with this system are in [13]. For the present data we use only one module of the available Alfvén wave antenna separated 180° in the toroidal direction from the probe system. It is powered by the 4-phase rf generator, which has a nominal output power $P \leqslant 1$ MW in the frequency range $f = 3.0$–5.5 MHz. It provides rf pulses lasting 10 ms. The antenna module of TCABR allows us to excite Alfvén waves with a large spectrum of poloidal, m, and toroidal, n, mode numbers. The utilization of only one antenna module does not permit to excite a monochromatic spatial spectrum of Alfvén modes; different modes can be excited simultaneously and they can deposit rf power in different plasma radial regions. In this work, we analyse discharges with rf waves of 40 kW, 3.6 MHz, and exciting dominant mode $m/n = 1/4$. Although these discharges have low efficiency of rf current drive and heating and the plasma bulk parameter changes are not noticeable, they are convenient for this work because the excited waves do not penetrate much in the plasma, interacting with the boundary plasma and modifying the plasma scrape-off layer. This interaction changes some measured plasma edge parameters slightly, mainly the temperature and the floating plasma potential. Thus, the turbulence spectrum modifications studied in this work could be partially caused by these parameter changes, an indirect effect of changes in the edge plasma conditions caused by the rf wave. On the other hand, analysing the time dependence of the changes during the rf pulse, we see evidence that the turbulence correlates with the wave amplitude, an indication of a direct effect of these waves themselves.

In the scrape-off layer, at $r/a = 1.17$, the values of density, temperature and plasma potential without rf injection are $n_e \approx 7.5 \times 10^{17}\,\mathrm{m}^{-3}$, $T_e \approx 6$ eV, and $V_p \approx 17$ V; with rf injection those values change to $n_e \approx 8.3 \times 10^{17}\,\mathrm{m}^{-3}$, $T_e \approx 14$ eV, and $V_p \approx 34$ eV. At the same position the relative level of fluctuations is $\tilde{n}/n_e \approx 0.30$ and $e\tilde{V}/kT_e \approx 0.45$ without and $\tilde{n}/n_e \approx 0.50$ and $e\tilde{V}/kT_e \approx 0.70$ with rf injection. A sample of part of the time series for fluctuating floating potential and ion saturation current with and without rf injection is given in figure 1. We note that the signals have a high frequency part and a burst sequence. Some characteristic plasma parameters (plasma current I_p and the central linear density n) and the power of rf injection for the data analysed are displayed in figure 2.

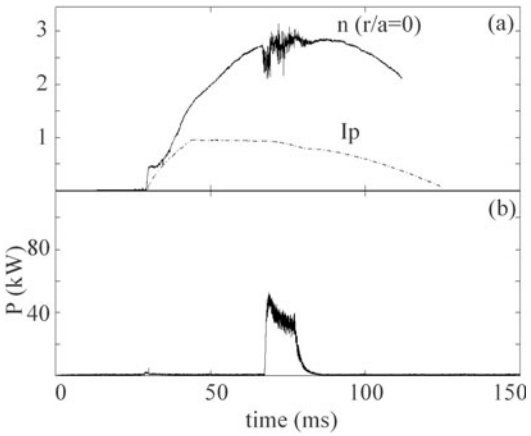

Figure 2. Typical profiles for the analysed discharges. Linear density n ($\times 10^{19}$) m^{-3} and plasma current I_p ($\times 10^5$) A (*a*); power of rf injection (*b*).

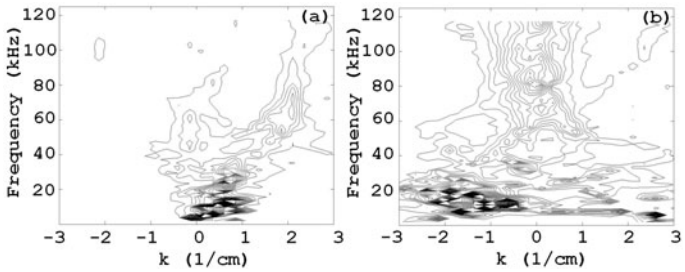

Figure 3. Contour plot of the wavelet $S(k, f)$ spectrum for potential fluctuations without (*a*) or with (*b*) rf injection, for chosen time intervals of 1.02 ms of the discharge. The figures have the same normalization levels.

3. Power spectra characteristics

Our characterization of turbulence is based on digital correlation techniques applied to floating potential and ion saturation current fluctuations. To examine the time behaviour of the fluctuations we split the data into segments of 1024 data points (≈1.02 ms) and apply the wavelet analysis to each segment.

We use wavelet analysis [20–22], that permits the time resolution of short interval data, convenient to investigate any possible fluctuation alteration during each single discharge. In these analyses we use the continuous wavelet transform based on the Morlet wavelet and the technique applied is the same used in [18]. Figure 3 presents the contour plot of the wavelet $S(k, f)$ spectrum [19] of the measured potential fluctuations, at a given radial position ($r/a = 1.17$) for $B_t = 1.1$ T, for a discharge, before (*a*) and during (*b*) the rf power injection. Frequency spectra are broad and extend up to 120 kHz. The fluctuation level increases with rf injection. With power injection, we observe the transfer of maximum power of frequency components from the positive to negative wavenumbers, especially in the scrape-off layer. As we can see from figure 3, even though the two-point technique used does not give precise slopes of the spectra, it is useful to recognize the change in the wave vector direction.

To observe the effect on the poloidal phase velocity for different values of the injected power, we present in figure 4 the data at the same radial position, from discharges with the

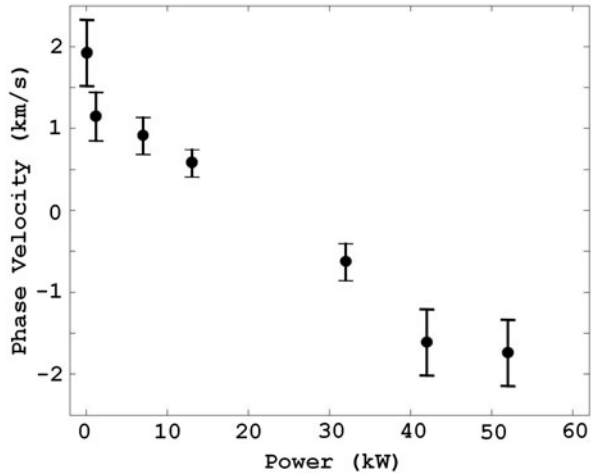

Figure 4. Dependence of poloidal phase velocity on the rf power injection for potential fluctuations at $r/a = 1.17$.

same density and plasma current, but with varying levels of injected power from 0 to 50 kW. We see that a minimum value of the injected power is necessary to change the direction of most frequency components. However, we note a saturation in this change for the two highest values. We also observe changes introduced in turbulence for different values of the plasma density and a fixed value of power injection (40 kW). The change in phase velocity direction is enhanced for lower densities; in fact at $r/a = 1.00$ (higher density) this effect is not noticeable. These results for phase velocity and its direction reversal, obtained by using the two-point technique, are confirmed by the use of a direct correlation technique. Moreover, this phase velocity change appears with the increase of the electric field with the rf wave, discussed in section 4.

To detect evidence of phase coupling between wavelet components of different scale lengths, possibly present in turbulence [20, 21], we combined wavelet and bispectral analyses by calculating wavelet bispectra and bicoherences between two frequencies, f_1 and f_2, and their sum or difference frequencies [18, 20–23]. To better identify the mode coupling, we calculated, for each segment of 1.02 ms, the summed bicoherence for all f_1 and f_2 satisfying the resonant condition $f = f_1 + f_2$. The numerical values of the summed bicoherence depend on the chosen calculation grid. Our frequency grid is of 256 points from 0 to 1 MHz, with a frequency cell of 3.9 kHz. Figure 5 shows the superposition of the summed bicoherence, at $r/a = 1.00$, for a chosen time interval of 1.02 ms, for potential fluctuations without or with rf injection. The tendency of power injection is to damp the defined frequency peaks and broaden the frequency range, i.e. it redistributes non-linear couplings among a much larger number of modes. Moreover, to verify the temporal behaviour of the observed coupling during the plasma discharge, we calculated the total bicoherence (integrated in f) for each mentioned segment. Thus, we concluded that the non-linear coupling between three waves is significantly affected by the rf wave, because the previous observed peaks disappear and the non-linear coupling becomes equally distributed over a broader frequency range.

4. Particle transport

To verify the rf injection influence on the total particle flux at the scrape-off layer during a discharge, we study the temporal heterogeneity of transport. We estimated this transport

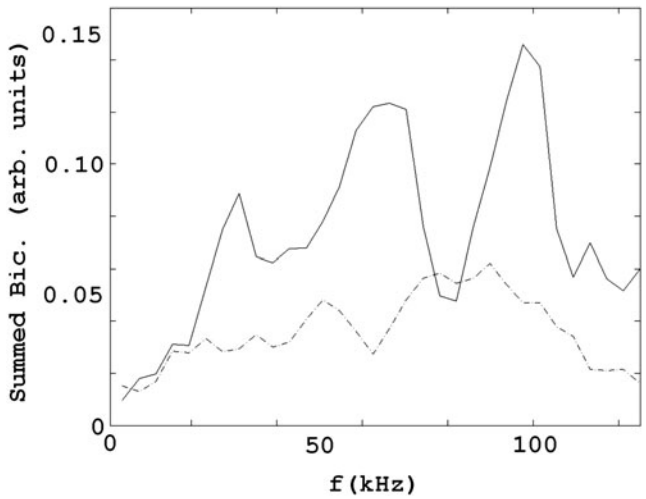

Figure 5. Superposition of the summed bicoherence without (——) or with rf injection (- - - -), for a chosen time interval of 1.02 ms, for potential fluctuations at $r/a = 1.00$.

from the electrostatic fluctuations analysed in this work. The radial particle flux, $\Gamma = \langle \tilde{n}\tilde{v}_r \rangle$, driven by the density and plasma potential fluctuations, $\tilde{n}$ and $\tilde{V}$, was obtained by calculating the fluctuating radial drift velocity $\tilde{v}_r = \tilde{E}_\theta / B_\mathrm{t} (\tilde{E}_\theta = k\tilde{V})$. In this section we used spectral analysis to calculate Γ from the equations [22]

$$T_r(f) = \frac{2k|S_{\tilde{n}\tilde{v}}| \sin(\theta_{\tilde{n}\tilde{v}})}{B_\mathrm{t}} \tag{1}$$

$$\Gamma = \int_0^\infty T_r(f)\,\mathrm{d}f \tag{2}$$

where k is the plasma potential poloidal wave number, $S_{\tilde{n}\tilde{v}}$ and $\theta_{\tilde{n}\tilde{v}}$ are the wavelet cross spectrum and the phase angle between the density and potential fluctuations, and B_t is the toroidal magnetic field.

Figure 6 shows the variation of the turbulence driven particle flux (integrated in frequency) for a discharge in time intervals of 1.02 ms before, during (between dashed lines) and after the power injection, for two radial positions, $r/a = 1.00$ and 1.17. Particle transport increases with the rf injected. The observed transport increases at the limiter position and this seems to be related to the increase in the fluctuating poloidal electric field shown in figure 7. This figure shows the formation of a poloidal electric field, at the plasma boundary, during the rf application. Moreover, the fluctuating radial electric field can be obtained by estimating the difference in the plasma potential (calculated from the floating potential and the electron temperature measurements) at two identical radial positions, $r/a = 1.00$ and 1.17. Thus, we observe that in the scrape-off layer the radial component increases with the rf wave. This field increase may be due to the fast electron loss caused by the rf wave. In this experiment, the transport increases with the drift flow resulting from $E_r \times B$. So, the increase of drift flow would explain the observed transport increase in the scrape-off layer. This supposition is similar to the one presented to interpret the plasma transport and drift flow reduction attributed to drift flow resulting from application of lower hybrid waves [25].

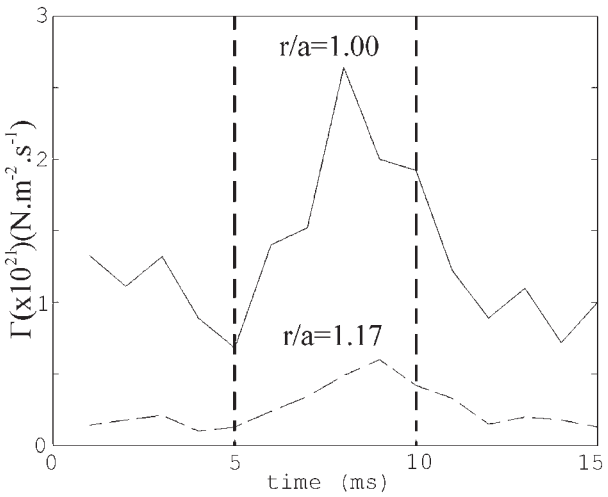

Figure 6. Evolution of turbulence driven particle transport for a discharge; before, during (between dashed lines), and after rf injection, at $r/a = 1.00$ and 1.17.

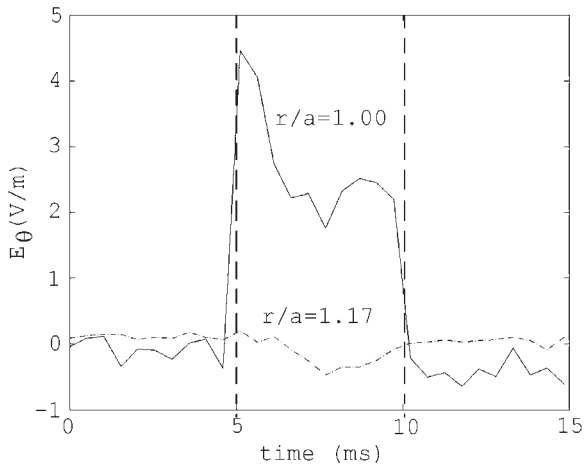

Figure 7. Estimation of poloidal electric field ($\times 10^3$) time evolution with rf injection (between dashed lines), for two radial positions.

5. Intermittent bursting

Non-diffusive transport caused by intermittent bursts in fluctuations in the plasma boundary region have been recorded in nearly all confinement devices with different plasma configurations [4–10]. One way to identify this kind of transport is through an analysis of fluctuation statistics. In this section we study the burst behaviour in the scrape-off layer to look for evidence of convective transport and compare this burst transport in the regimes without or with the same rf perturbation.

Figure 8 shows a histogram of the absolute value of turbulent ion saturation fluctuation amplitudes for the two plasma conditions, without (*a*) or with (*b*) rf at $r/a = 1.00$. The presence of the rf perturbation enhances the net tendency towards a positive skewed distribution.

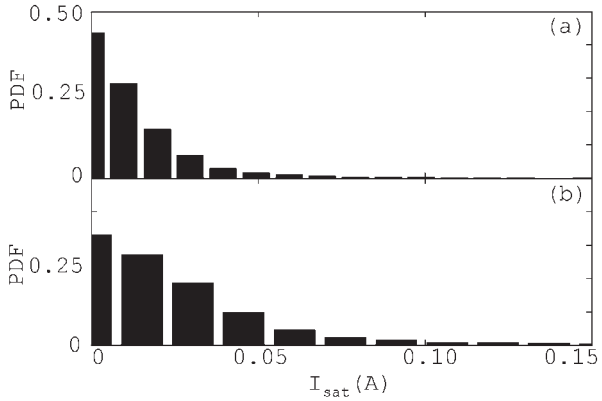

Figure 8. Normalized histograms of the absolute value of ion saturation fluctuation amplitudes without (*a*) or with (*b*) rf injection at $r/a = 1.00$.

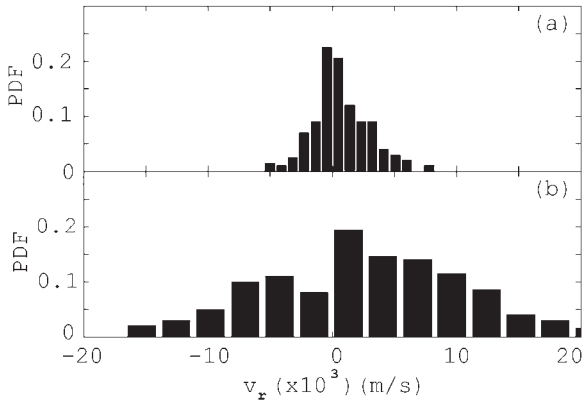

Figure 9. PDF for the radial velocity fluctuations of burst events without (*a*) or with (*b*) rf application at $r/a = 1.00$.

Moreover, to estimate the relative importance of the fluctuation peaks in terms of the turbulence intensity contained in them, we determine the intermittent burst's total intensity and compare it with the overall one. In this work, we obtain a good discrimination of the bursts by selecting the fluctuating density with amplitudes equal to or greater than 2.0 times the fluctuation standard deviation. We also calculate the histograms of the laminar time between two successive bursts [26]. Although, for the convenient chosen high thresholds, the statistics is low and the value distribution is broad, it is possible to conclude that these histograms are neither peaked nor Gaussian, with a most probable value around 75 μs. We note that the histogram does not change much for the two cases.

To obtain the burst radial velocity, v_r, we take as usual the difference between the floating potentials of the two poloidally separated tips where bursts are pinpointed on the density fluctuation signal. Figure 9 shows the radial velocity histogram of the bursts for the two plasma conditions, without (*a*) or with (*b*) rf application at $r/a = 1.00$. The PDF for the radial velocity is positively skewed in figure 9(*b*), indicating outward average flux accentuated by rf injection. The mean radial velocity in the regime without rf at $r/a = 1.00$ takes a value close to $5 \times 10^2\,\mathrm{m\,s^{-1}}$ and decreases with r. The same reduction is observed in the case of

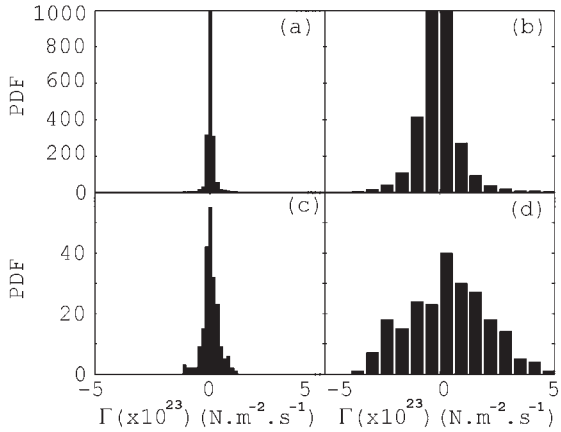

Figure 10. Histograms of total particle transport without (*a*) or with rf perturbation (*b*). Histograms of burst particle transport without (*c*) or with rf injection (*d*), at $r/a = 1.00$.

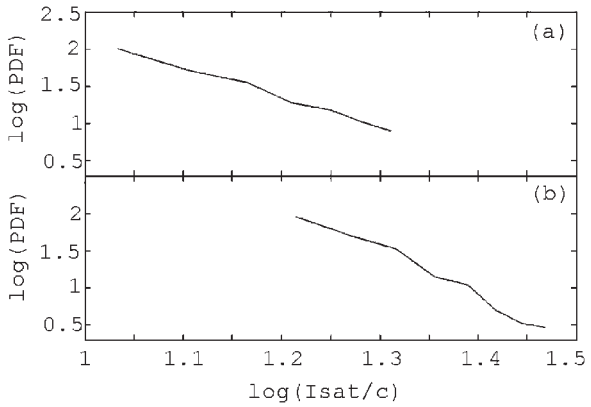

Figure 11. Logarithmic plot of the frequencies of ion saturation current bursts, as a function of their normalized amplitudes (Isat/c), before (*a*) and after (*b*) the rf perturbation, at $r/a = 1.00$.

rf perturbation for which the mean radial velocity is $2 \times 10^3\,\mathrm{m\,s^{-1}}$ at $r/a = 1.00$. Thus, we find a significant increase of radial velocity with the rf injection.

The total (laminar and bursting) radial particle transport for the fluctuations is also calculated directly from data multiplying the obtained radial velocity by the simultaneous fluctuating density, both obtained every 1 μs. Thus, figure 10 shows histograms of this transport at $r/a = 1.00$ without (*a*) or with rf injection (*b*). The same is calculated for the bursts shown in figure 10 without (*c*) or with rf injection (*d*). From these figures, we calculated the ratio R_Γ of the burst transport to the overall one. At all measured radial positions, the burst contributions without and with perturbation are about 20% and do not change much with the rf perturbation. Furthermore, the time ΔT occupied by the bursts, normalized to the time series, is about 3% and remains almost the same for all the mentioned conditions.

From figure 8 we see that the probability distributions of fluctuating ion saturation current have long tails that characterize a typical flight distribution [27, 28]. Thus, we associate the high peaks to rare events described as flights. To further explore this association we present in figure 11 the logarithmic plot of the probability density function as a function of

the ion saturation current burst amplitude before (a) and during (b) the rf injection, for data at $r/a = 1.00$. Supposing that these distributions are power laws, varying as $I_s^{-\rho}$, we obtained decay coefficients $\rho \approx 2.0$ without and $\rho \approx 3.5$ with rf perturbation. The same values are obtained for the decay coefficients at the position $r/a = 1.17$.

6. Conclusions

We report the main spectral properties of the scrape-off layer electrostatic turbulence and transport in the TCABR tokamak. For the chosen excitation conditions, with rf injection, the power spectra of electrostatic fluctuations change, mainly their amplitudes and phase velocities. The background fluctuation amplitude increases and, for high enough rf power, the average phase velocity reverses its direction. The three waves coupling, given by the phase bicoherence, decreases with the applied perturbation. For some frequencies, the coupling is high before the rf wave injection, with sparse coherent structures. After the injection, the non-linear coupling becomes equally distributed over the frequency range. This coupling dependence was also observed for the coherent structures observed in ADITYA tokamak [29]. Furthermore, for the same data, structures identified with a time multiscaling analysis are destroyed by the rf wave injection [30, 31].

The total transport driven by the electrostatic wave turbulence increases with the rf power. A lesser but significant part of this transport (about 20%) is radially convected by the intermittent fluctuation bursts.

We compile statistics on burst amplitude to determine the probability of fluctuating ion saturation current peaks. The long tail of these probability distributions resembles a flight distribution and the high peaks are associated to the flights. The decay coefficient of the probability density function increases with the rf, i.e. the long flights (high amplitude peaks) are less frequent. Thus, the variety and intermittency of bursts decrease. Recently, evidence of Levy flights associated with the intermittent amplitude bursting of the electrostatic plasma turbulence were found by using a modified method of fractiles [32].

Although we cannot identify the driving instability that creates these turbulence bursts, our conclusions support the existence of plasma structures called blobs, a term introduced to denote concentrations of plasma density, encountered intermittently in the scrape-off-layer with high radial velocities [6]. We find evidence that these blobs contribute to the radial transport. Furthermore, they are part of the flight statistics that describes the scrape-off-layer turbulence consisting of the background fluctuations and the intermittent bursts [32]. Finally, we would like to mention that our work supports the conclusion that the increase in bursting amplitudes (associated with propagating structures) should increase the particle transport [33].

Acknowledgments

The authors are indebted to the TCABR team for the use of laboratory facilities and acknowledge the referees' suggestions. This work was partially supported by the Brazilian governmental agencies FAPESP (Fundação de Amparo à Pesquisa do Estado de São Paulo), CNPq (Conselho Nacional de Pesquisa) and CAPES (Fundação Coordenação de Aperfeiçoamento de Pessoal de Nível Superior).

References

[1] Wootton A J, Carreras B A, Matsumoto H, McGuire K, Peebles W A, Ritz Ch, Terry P W and Zweben S J 1990 *Phys. Fluids* B **2** 2879

[2] Wagner F and Stroh U 1993 *Plasma Phys. Control. Fusion* **35** 1321
[3] Terry P W 2000 *Rev. Mod. Phys.* **72** 109
[4] Boedo J A *et al* 2001 *Phys. Plasmas* **8** 4826
[5] Antar G Y, Devynck P, Garbet X and Luckhardt S C 2001 *Phys. Plasmas* **8** 1612
[6] Antar G Y, Krashennikov S I, Devynck P, Doerner R P, Hollmann E M, Boedo J A, Luckhardt S C and Conn R W 2001 *Phys. Rev. Lett.* **87** 065001
[7] Gulke O *et al* 2001 *Phys. Plasmas* **8** 5171
[8] Antoni V *et al* 2001 *Phys. Rev. Lett.* **87** 1
[9] Antoni V *et al* 2001 *Europhys. Lett.* **54** 51
[10] Vianello N *et al* 2002 *Plasma Phys. Control. Fusion* **44** 2513
[11] Horton W 1999 *Rev. Mod. Phys.* **71** 735
[12] Ruchko L F, Ozono E, Galvão R M O, Nascimento I C, Degasperi F T and Lerche E 1998 *Fusion Eng. Des.* **43** 15
[13] Ruchko L F *et al* 2002 *Braz. J. Phys.* **32** 57
[14] Litwin C, Hershkowitz N, Wukitch S, Intrator T, Vucovic M, Brouchous D, Breun R and Harper M 1995 *Phys. Plasmas* **2** 4551
[15] Mantica P, Vayakis G, Hugill J, Cirant S, Pitts R A and Matthews G F 1991 *Nucl. Fusion* **31** 1649
[16] Richards B *et al* 1994 *Phys. Plasmas* **1** 1606
[17] Le Blanc *et al* 1999 *Phys. Rev. Lett.* **82** 331
[18] Ferreira A A, Heller M V A P and Caldas I L 2000 *Phys. Plasmas* **7** 3567
[19] Levinson T, Beall J M, Powers E J and Bengtson R D 1984 *Nucl. Fusion* **24** 527
[20] Van Milligen B Ph, Sánchez E, Estrada T, Hidalgo C, Brañas B, Carreras B and L García 1995 *Phys. Plasmas* **2** 3017
[21] Van Milligen B Ph, Hidalgo C, Sánchez E, Pedrosa M A, Balbín R, García-Cortés I and Tynan G R 1997 *Rev. Sci. Instrum.* **68** 967
[22] Heller M V A P, Brasilio Z A, Caldas I L, Stockel J and Petrzilka J 1999 *Phys. Plasmas* **6** 846
[23] Ritz Ch P, Powers E J and Bengston R D 1989 *Phys. Fluids* B **1** 153
[24] Galvão R M O *et al* 2001 *Plasma Phys. Control. Fusion* **43** A 299
[25] Ding B J, Kuang G L, Song M, Xu G S, Wan B N, Zhao Y P and Li G 2004 *Phys. Plasmas* **1** 207
[26] Spada E *et al* 2001 *Phys. Rev. Lett.* **86** 3032
[27] Solomon T H, Weeks E R and Swinney H L 1994 *Physica* D **76** 70
[28] Shlesinger M F, Zaslavsky G M and Frisch U (ed) 1995 *Lévy Fligths and Related Topics in Physics* (Berlin: Springer)
[29] Jha R, Mattoo S K and Saxena Y C 1997 *Phys. Plasmas* **4** 2982
[30] Baptista M S, Caldas I L, Heller M V A P and Ferreira A A 2002 *Physica* A **301** 150
[31] Baptista M S, Caldas I L, Heller M V A P and Ferreira A A 2003 *Phys. Plasmas* **10** 1283
[32] Chechkin A V, Gonchar V Yu and Szydlowski M 2002 *Phys. Plasmas* **9** 78
[33] Martines E, Hron M and Stöckel J 2002 *Plasma Phys. Control. Fusion* **44** 351